Morphology and ionic conductivity of complexes of sodium iodide and sodium thiocyanate with poly(ethylene oxide)

C. C. Lee* and P. V. Wright
Department of Ceramics, Glasses and Polymers, The University of Sheffield, Elmfield, Northumberland Road, Sheffield S10 2TZ, UK
(*Received* 30 *March* 1981)

Morphological and differential thermal analysis (d.t.a.) studies show that the melting temperature of the principal crystalline lamellar phase (phase I) of PEO–NaI and PEO–NaSCN complexes (which is ~463K for a high polymer) is independent of the nature of the anion. However, n.m.r. and conductivity measurements indicate that mesophase behaviour occurs in phase I above ~333K in NaSCN–PEO and ~363K in NaI–PEO. This temperature region marks the onset of an ionic conduction process of lower activation energy. The disordering of a second complexed phase (phase II) which forms in the interlamellar regions of the linear complexes and within the network of a crosslinked PEO gel is considered to account for the 325–340K endotherms which are observed in these materials. In particular, annealed and melt recrystallized NaSCN complexes with high molecular weight PEO form banded morphological features consisting of stacks of lamellar fragments which are indicative of rigid and stable molecular units. The ionic conductivities of saturated (excess salt) and stoichiometric linear complexes are compared with that of the complexed network which has the greater ambient temperature conductivity.

Keywords Poly(ethylene oxide); sodium; complex; morphology; mesophase; conductivity

INTRODUCTION

Since the crystalline complexes of poly(ethylene oxide) PEO with ammonium and alkali metal salts were first reported[1] they have aroused some interest for possible applications as solid electrolytes[2,3] in which the conduction is considered to arise from essentially cationic migration[3].

Here, we report investigations into the morphology of the crystalline complexes with sodium iodide and sodium thiocyanate with some morphological implications for ionic conductivity in these materials. Considerations of the molecular structure of these and similar complexes are reserved for a separate paper[4].

The crystalline complexes have a stoichiometry of 1 mole alkali metal salt with 4 moles ethylene oxide unit (EO) although samples having excess and deficient salt are also considered.

EXPERIMENTAL

NaSCN and NaI (standard laboratory grade) were oven dried at 573K removing water of crystallization from the NaSCN. PEO fractions with molecular weights 600 to 5×10^6 were supplied by British Drug Houses Ltd. with the exception of PEO 10 000 and PEO 20 000 which were donated by Hoechst Chemicals and Union Carbide UK Ltd., respectively.

Complexes were prepared by dissolution of the appropriate molar proportions of salt and EO units of polymer in methanol. When the solutions were homogeneous the solvent was removed using a vacuum pump. Annealed samples were prepared by sealing the material under vacuum in glass tubes which were then held at the required temperature in a heated aluminium block fitted with a thermostatic control.

A PEO 600–maleate gel was prepared by reacting equimolar quantities of poly(ethylene glycol) 600 with maleic anhydride. After a preliminary condensation reaction at 373K under a N_2 atmosphere, vacuum was applied and the reaction temperature gradually raised to 403K. The gel was crosslinked at 373K using 5% benzoyl peroxide initiator. The salt was introduced into the gel by immersing in saturated solutions of chloroform–diethyl ether for several days. After vacuum removal of solvents the samples were finally cut into shape for conductivity measurements removing surface salt crystals. The salt content was determined by flame photometry on aqueous solutions prepared by leaching of salt from small fragments of surface cleaned gel. The stoichiometry of the gels was found to be approximately 1 mole salt per 6 moles EO unit.

Conductivity measurements on crystalline samples were made by first compressing the complexes between platinum foil electrodes into pellets 1.3 cm in diameter and up to 0.6 cm in thickness using a 10 ton hydraulic press. Electrode adhesion and overall contact were optimized by smearing the electrode at its interface with the sample with a low molecular weight PEO (200–400) complex with the appropriate salt before pressing. The pellets were mounted between cylindrical copper contacts of the same diameter in sealed tubes containing phosphorus

* Present address: Waters Associates, Singapore.

0032-3861/82/050681-09$03.00
©1982 Butterworth & Co (Publishers) Ltd.

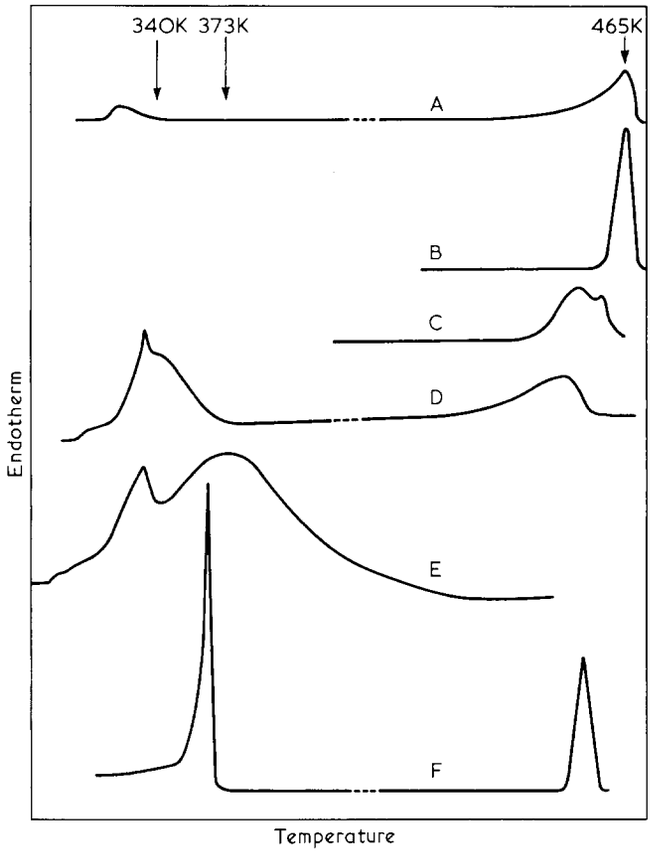

Figure 1 D.t.a. traces of PEO complexes: A, PEO 10 000–NaSCN (1 : 4 stoichiometry) – first cycle; B, PEO 10 000–NaI (1 : 4 stoichiometry) – first cycle; C, PEO 300 000–NaI (1 : 4 stoichiometry) – second cycle; D, PEO 600 000–NaI excess salt (1 : 3 stoichiometry) – first cycle; E, PEO 600–maleate gel–NaI (~1 : 6 stoichiometry); F, PEO 600 000–NaI (1 : 4 stoichiometry) – first cycle. Heating rates are 1K min^{-1} except (D) 340K endotherm only, 10K min^{-1}; (E) 6K min^{-1} and (F) 3K min^{-1}

pentoxide as drying agent. The tubes were heated in a thermostatically-controlled aluminium block. Conductivity measurements were made at frequencies over the range 10^2–10^5 Hz using a Lynch bridge[5].

Transmission electron microscopy was performed using a Hitachi HU 11A electron microscope. The samples were fractured under vacuum inside the bell jar of an AEI Metrovac type 12 coating unit and ~50 Å thickness of carbon was deposited onto the fracture surfaces. The replica was floated on water onto a copper grid. After a preliminary examination under the electron microscope the replica was returned to the coating unit for shadowing at an angle of ~45° using 40/60 Pd/Au alloy to enhance the image contrast.

Differential thermal analysis (d.t.a.) was performed using a Stanton Redcroft model 673–4 and a Stanton Redcroft model 671. The cell of the latter was fitted with drying tubes containing P_2O_5 and could be cooled using liquid N_2. Samples were run in air at atmospheric pressure. Peak areas were calibrated using the melting exotherms of benzil, benzoic acid and quinol.

Nuclear magnetic resonance (n.m.r.) spectroscopy was performed on a Japan Electron Optic Lab. 60 MC spectrometer fitted with a variable temperature probe. Samples for n.m.r. analysis were sealed inside glass tubes under a vacuum of better than 0.1 Torr. Spectra were obtained at temperatures up to 443K.

DISCUSSION

Figure 1 shows d.t.a. traces of NaI and NaSCN complexes with poly(ethylene oxide). The highest temperature endotherms (~463K for complexes with high molecular weight polymer) coincide with the disappearance of birefringence from the samples and indicate the melting of crystalline lamellae. Samples of NaSCN complexes annealed close to the peak melting temperature have typically broad asymmetric melting endotherms whereas those of NaI samples with 1:4 stoichiometry are narrower and more symmetrical. However, unannealed samples of NaI complexes may show several peaks or shoulders corresponding to several morphological states and those prepared with a stoichiometric excess of NaI have broader melting endotherms which resemble those of NaSCN complexes.

Lamellar thickening in solution-deposited samples

D.t.a. data for PEO complexes with both NaI and NaSCN are given in *Tables 1* and *2*. The samples have 1:4 stoichiometry (Na^+:EO) except where indicated. Figures within square brackets indicate temperature (K) and time (h) of annealing, respectively. *Table 1* contains melting temperatures in successive d.t.a. cycles. The first number in each column represents the melting temperature of solution-deposited material either untreated or annealed without passing through the melting range with the exception of the case where 'melt' denotes recrystallization from the melt.

With the exception of PEO 600 complexes, each type of complex with the same PEO molecular weight has essentially the same melting temperature. This suggests that a common sodium ion–PEO adduct is the predominant feature in determining the stability of the complexes in the region of the melting temperatures. Whereas PEO 600 complexes may be exceptional in having structures similar to those described by Weber *et al.*[6] for oligomeric complexes, the remainder presumably have the same helical conformations of the PEO chains complexed to sodium ions, with peak melting temperatures essentially independent of the nature of the anions.

Annealing of the solution-deposited PEO 10 000–NaI

Table 1 Melting temperatures of PEO complexes in successive d.t.a. cycles

PEO fraction	NaI complexes (K)	NaSCN complexes (K)
600	380	407, 393
1000	419.4, 418.8	423.4, 423.6
1500	433.0, 431.3	437.2, 439.0
4000	455.4, 452.0	456.0, 456.0
6000	461.6, 458.2	460.5, 461.2
10 000	465.0, 460.0	463.5, 464.2
20 000	461.1, 457.0, 455.0	461.0, 459.9
5×10^6	463.4, (463.3), 460.0	464.8, 465
6×10^5 [453, 167]	465.9	467
6×10^5 [456 melt, 151]	457	
6×10^5, 1 : 6 stoichiometry	464.4	
6×10^5, 1 : 3 stoichiometry [343, 330]	456.5	

Stoichiometry is 1 : 4 except where indicated. Numbers in square brackets indicate annealing temperature (K) and time (h), respectively. 'Melt' denotes melt crystallization. Figure in parentheses denotes subsidiary peak

Table 2 D.t.a. cycle data for PEO 10 000 and PEO 20 000 complexes

	T_{m1}	ΔS_{m1} (J [mole EO]$^{-1}$ K^{-1})	T_{max1}	T_{c1}	T_{m2}	T_{max2}	T_{c2}
PEO 10 000–NaI [453, 24]	465.0	25.4	467	424	456.3	461	432
PEO 10 000–NaI [453, 164]	467.2		477	420	458.8	461	432
PEO 10 000–NaSCN [426, 24]	465.2	27.1	470	430	464.5	477	439
PEO 10 000–NaSCN [433, 24]	465.0	21.2	467	442	464.2	493	439 (430)
PEO 20 000–NaI	461.1		464	428	457.0	464	428
PEO 20 000–NaSCN	461.0		467	426	459.9	463	428
PEO 20 000–NaSCN [453, 72]	464.0		473	428			
PEO 10 000	337.0	25.9					

Heating and cooling rates, 1K min^{-1}; other details as in *Table 1*

and NaSCN complexes for moderate times (~24 h) at temperatures above the threshold of the melting region (i.e. above ~430K for NaSCN samples and above 450K for NaI samples) gives first cycle peak melting temperatures of ~465K which are the same as those of unannealed samples. However, the closest striations on electron micrographs of unannealed solution-deposited complexes or of complexes annealed well below the melting regions (see *Figures 2a*, *2e*, *3a*, *3c* and *3d*) show that the lamellar thicknesses of 150–200 Å are significantly less than those of the complexes annealed close to melting temperatures (see *Figures 2b*, *2f*, *3b* and *3d*) which are 400–500 Å for PEO 10 000 complexes and about 600 Å for the high molecular weight PEO complexes. Therefore, in the solution-deposited PEO 10 000 samples lamellar thickening occurs rapidly in the d.t.a. instruments at heating rates of ~3K min^{-1} at temperatures close to the peak melting temperatures.

At higher heating rates, the melting of unthickened morphologies of PEO 6000 and 10 000 may be observed by taking into account the superheating (~5K for thickened lamellae and ~2K for unthickened lamellae) at 6K min^{-1} with the instrument used in the present work, while PEO 20 000 complexes fail to thicken to the extent of the PEO 10 000 complexes without annealing for extended periods at ~453K. However, NaI complexes annealed at 343K in the presence of a stoichiometric excess of NaI give reduced melting temperatures (see *Table 1*). At 343K ionic diffusion is pronounced, as discussed below, but large scale chain motion is not evident. Whether the annealing process has effected an erosion of the crystalline lamellae or simply consolidated the solution-deposited morphology is not clear. However, the observation suggests that the suppression of vacancies in the ionic lattice from the reservoir of excess salt may be effective in suppressing lamellar thickening in NaI samples and that conversely, the nominally 1:4 stoichiometric solution-deposited samples include sufficient lattice vacancies to permit the observed high chain mobility prior to melting.

However, similar retardation of lamellar thickening rates in the presence of excess salt is not observed in NaSCN complexes. Samples prepared with deficient salt give broad based melting peaks but have peak maxima at temperatures characteristic of thickened material.

Melting temperature–morphological correlations

As *Figures 2b* and *3b* show, thickened lamellae of the PEO 10 000 complexes have thicknesses approximating to the number-average expected value of 411 Å for extended-chain helical macroconformations in which four EO units extend over the observed[4] fibre repeat distance of 7.23 Å.

The assignment of all first cycle melting temperatures of complexes with PEO 1000–10 000 to extended-chain morphologies may be rationalized according to the Flory theory as applied by Booth and coworkers[7] for pure PEO fractions:

$$T_m = T_m^0\left[1-\frac{2\sigma}{(\Delta h)\zeta}\right]\Big/\left[1+\frac{R\,T_m^0}{\Delta h}\left(\frac{1}{\bar{X}}-\ln I\zeta\right)\right] \quad (1)$$

T_m^0 is the melting temperature of crystals of infinite length; σ_e is the end interfacial free energy; Δh is the heat of fusion and is taken to be 11.8 kJ mol^{-1} as obtained from calibrated d.t.a. melting peak areas of annealed PEO 10 000 complexes. $\bar{X}_n$ is the number-average degree of polymerization of the sample and I is the probability of choosing a sequence ζ units in length which does not contain a chain end.

A scheme, detailed elsewhere[8], which is at least internally consistent, is obtained by arbitrarily choosing $\sigma_e = 16.8$ kJ per mole of emerging chain for PEO 10 000 complexes as found by Booth and coworkers for pure PEO 10 000. This assignment renders $T_m^0 = 473$K. Good agreement between calculated and experimental melting temperatures is obtained if σ_e (ranging from 8.4 to 16.8 kJ mol^{-1}) and X_w/X_n (ranging from 1.2 to 1.5) are allowed to increase over the PEO molecular weight range 1000 to 10 000 thus following similar trends to those found for pure PEO fractions by Booth *et al.*

Extended annealing over 117 h at 453K of solution-deposited PEO 10 000–NaI gives rise to a higher melting endothermic peak or shoulder with a maximum at 467K. The electron micrograph of this material (*Figure 2c*) suggests that the higher melting fraction probably consists of paired extended-chain lamellae.

Annealing of solution-deposited high molecular weight PEO–NaI complexes gives rise to no notable morphological features other than the well-defined thickened lamellae shown in *Figure 2f*. However, annealing of solution-deposited high molecular weight PEO–NaSCN complexes at temperatures between ~438K and the melting temperature gives rise to the banded structures shown in *Figures 3e* and *3f*. The resemblance of these structures to very thick extended-chain lamellae (as found for example in melt re-crystallized polytetrafluorethylene or in polyethylene crystallized under high pressures and temperatures) is only superficial. The banded structures appear to be formed from stacks of lamellar fragments, some thickened, which had similar orientations to the initial

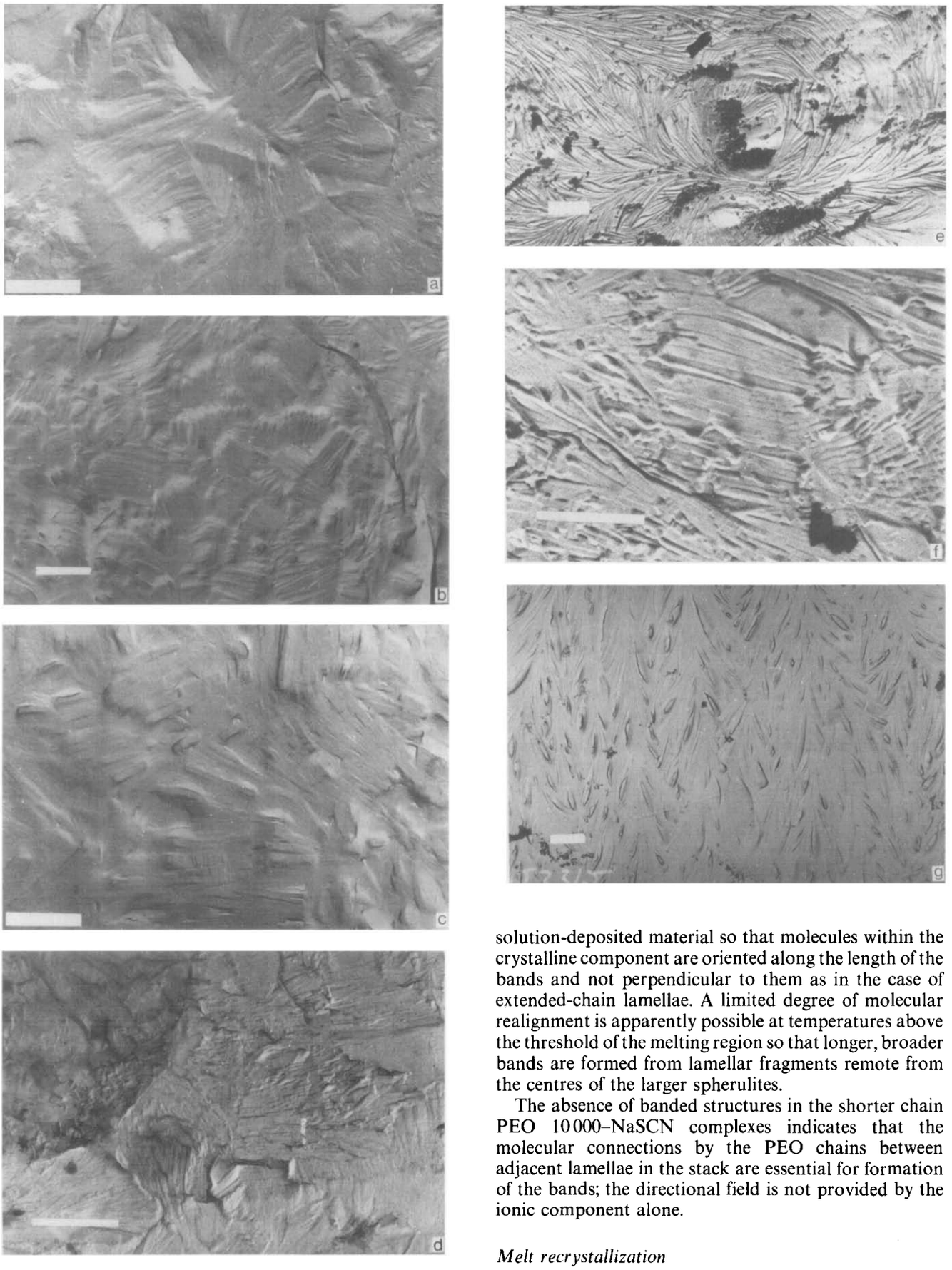

Figure 2 Electron micrographs of PEO–NaI complexes (scale bar 1 μm): (a) PEO 10000–NaI solution deposited; (b) PEO 10000–NaI [453, 24]; (c) PEO 10000–NaI [453, 117]; (d) PEO 10000–NaI [450M, 24] (melt recrystallized); (e) PEO 6×10^5–NaI [438, 133]; (f) PEO 6×10^5–NaI [457, 168]; (g) PEO 6×10^5–NaI melt recrystallized slowly cooled

solution-deposited material so that molecules within the crystalline component are oriented along the length of the bands and not perpendicular to them as in the case of extended-chain lamellae. A limited degree of molecular realignment is apparently possible at temperatures above the threshold of the melting region so that longer, broader bands are formed from lamellar fragments remote from the centres of the larger spherulites.

The absence of banded structures in the shorter chain PEO 10000–NaSCN complexes indicates that the molecular connections by the PEO chains between adjacent lamellae in the stack are essential for formation of the bands; the directional field is not provided by the ionic component alone.

Melt recrystallization

Table 1 shows that the initial high melting temperatures of the NaSCN complexes are retained in the second and subsequent d.t.a. cycles. However, for PEO–NaI complexes with PEO molecular weights of 4000 and above, recrystallization from the melt is followed by

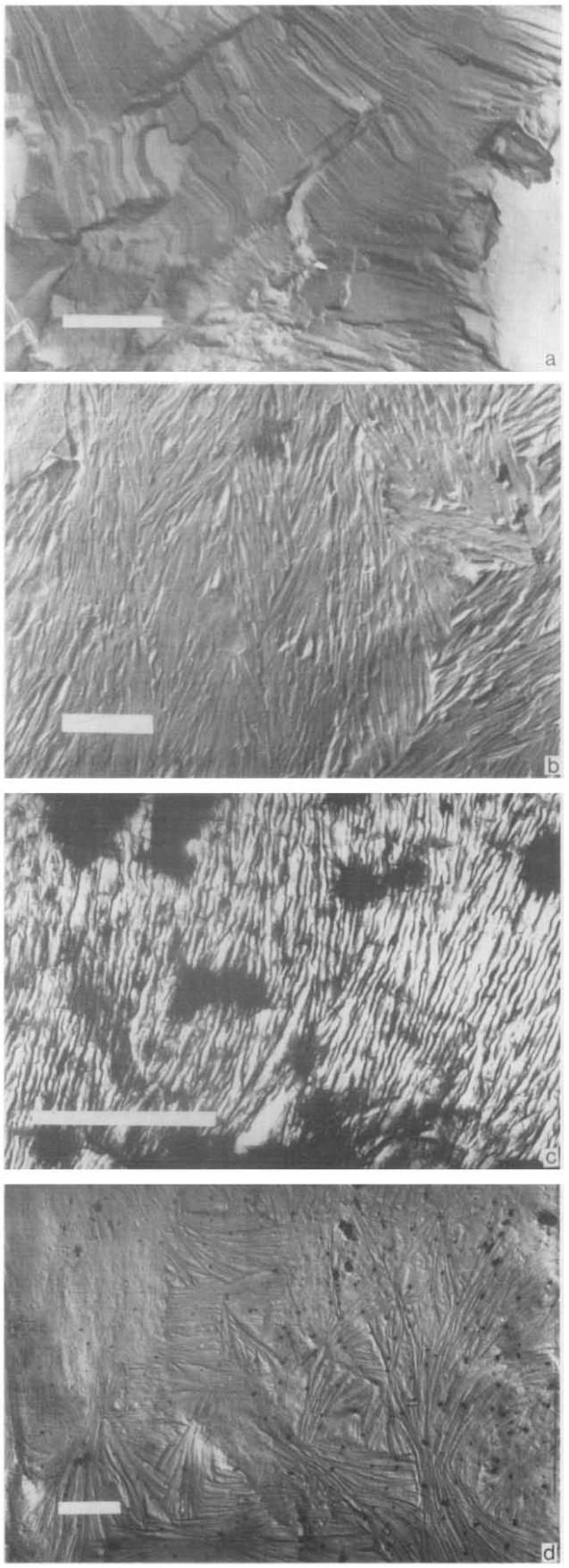

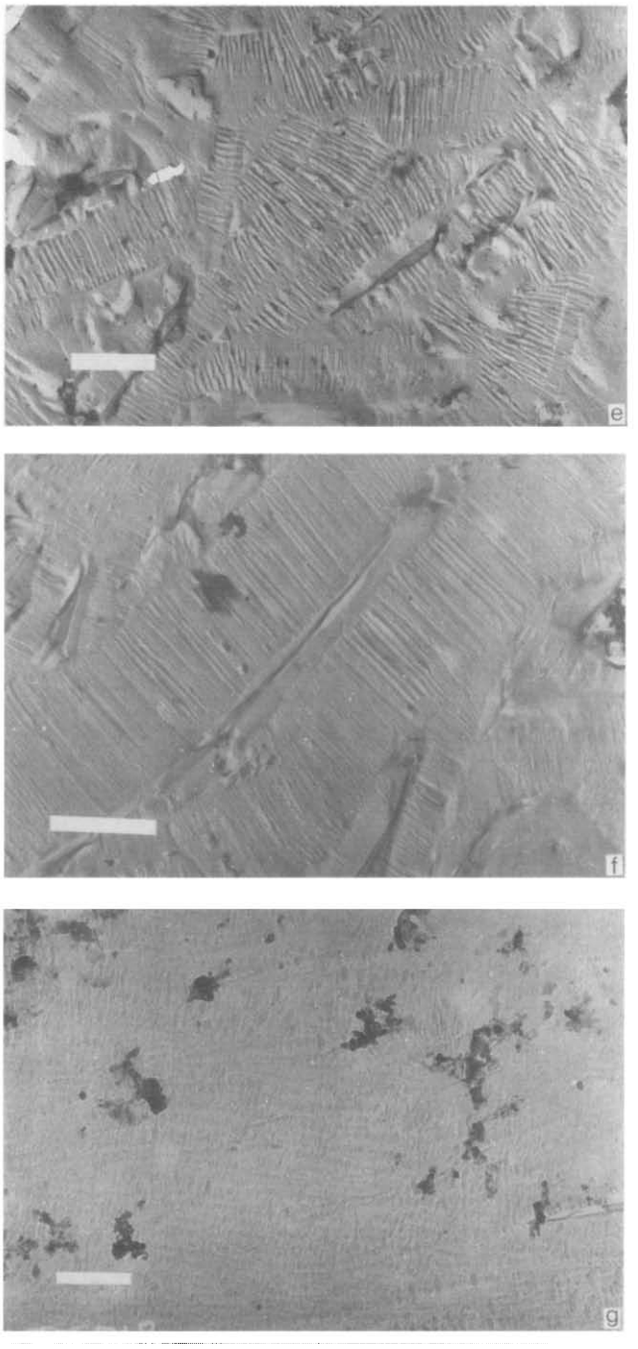

Figure 3 Electron micrographs of PEO–NaSCN complexes (scale bar 1 μm): (a) PEO 10000–NaSCN solution deposited; (b) PEO 10000–NaSCN [180, 48]; (c) PEO 6 x 10^5–NaSCN solution deposited; dark striations apparently arise from polymer adhering to the replica; (d) PEO 6 x 10^5–NaSCN [433, 168]; (e) and (f) PEO 6 x 10^5–NaSCN [458, 7]; (g) PEO 6 x 10^5–NaSCN [453 melt, 4]

fusion at reduced temperatures. The electron micrographs show that the reduced melting temperatures follow recrystallization with reduced lamellar thickness. For PEO 4000–NaI, PEO 6000–NaI and PEO 10000–NaI the reduced melting temperatures may again be rationalized using equation (1), by assigning discrete folded macroconformations with σ_e lowered by successive folds. Thus it is concluded that PEO 4000–NaI and PEO 6000–NaI fold once and PEO 10000–NaI forms once- and twice-folded macroconformations. PEO 20000–NaI increases its degree of folding with recycling and high molecular weight PEO–NaI samples similarly reduce their lamellar thickness progressively to about 200 Å, showing multiple melting peaks (see *Figure 1C*) before an apparent equilibrium morphology is obtained. Even extended annealing at 456K of melt recrystallized NaI–PEO samples failed to effect the thickening that occurs rapidly in 1:4 solution-deposited materials.

Melt recrystallized high molecular weight PEO–NaSCN is shown in *Figure 3g*. There is no evidence of spherulites, but the thickened lamellar fragments appear to be threaded together in a manner resembling the 'shish-kebab' structures formed from stirred solutions or strained melts.

These observations are consistent with typical mesophase behaviour in the PEO–NaSCN complexes at temperatures immediately prior to final melting. The complexed molecular units of PEO–NaSCN are apparently quite rigid and remain essentially intact on melting whereas those of PEO–NaI suffer some disruption.

The stability of the complex molecular units in the melt is reflected in the d.t.a. cycle data for some complexes with PEO 10000 and PEO 20000 given in *Table 2*. Despite some high melt temperatures, the recrystallization temperatures of PEO 10000–NaSCN samples are the highest suggesting that these complexes have the most ordered melts of rod-like molecular units which readily recrystallize to extended-chain lamellae. The melts of previously-folded macroconformations recrystallize at intermediate temperatures (426–432K). These are the T_{c2} for PEO 10000–NaI and both T_{c1} and T_{c2} for PEO 20000–NaSCN and PEO 20000–NaI. If a 'memory' of the lamellar macroconformations exists in the melt, the latter complexes would have molecules with smaller axial ratio and greater orientational freedom in the melt than do the extended-chain molecular units. The lowest recrystallization temperatures are the T_{c1} from melts of previously fully extended chains of PEO 10000–NaI which, at this stage, may include the most diverse assembly of conformational states.

Also shown in *Table 2* are some entropies of fusion for extended-chain complexes with PEO 10000 estimated from calibrated, first-cycle d.t.a. peak areas. This procedure gave good agreement with literature values for pure PEO. PEO 10000–NaSCN [426,24], annealed below the threshold of the melting range has the highest entropy of fusion, ΔS_1. This may reflect consolidation of some folded macroconformations resulting in incomplete thickening and a low value for T_{c1} in comparison with the other T_c for PEO 10000–NaSCN. A series of experiments[8] to determine entropy of fusion *versus* annealing temperature showed that the entropies of fusion of NaSCN complexes passed through a maximum at an annealing temperature of ~400K. NaI complexes also gave a maximum at this temperature but, following a minimum at ~420K, their entropies of fusion then increased with increasing annealing temperature up to the melting range. However, entropies of fusion for NaI and NaSCN complexes are generally no greater than that for pure PEO despite the additional ionic components. This observation is indicative of ordered melts and/or disordered crystals at the melting temperature.

Transformations prior to principal melting

The first baseline deflections on d.t.a. traces of all the sodium ion complexes appear between ~273 and 293K. This presumably represents the glass transformation region for the non-crystalline component of the complexes corresponding to the behaviour first reported by Moacanin and Cuddihy[9] for lithium perchlorate complexes with atactic poly(propylene oxide). However, both NaI and NaSCN complexes show further endotherms prior to principal melting. The observations may be summarized as follows.

(i) A well-defined first-order transformation is observed in d.t.a. traces of both NaI and NaSCN complexes. This endotherm is generally smaller than the principal melting peak with a peak maximum between ~325K and ~340K. It is observed for high molecular weight PEO and for PEO 6000 and PEO 10000 complexes with excess (1:3), stoichiometric (1:4) or slightly deficient (1:5) salt though it may be practically eliminated in annealed, stoichiometric samples or 'excess salt' samples of PEO 10000 and PEO 6000 complexes. Thus the endotherms at 325–340K may apparently be observed in samples having interlamellar chain connections but not in complexes of PEO 6000 or PEO 10000 having well-ordered extended or once- or twice-folded macroconformations.

These observations led to the suggestion that complexed structure may exist in the layer sandwiched between the crystalline lamellae[2]. Investigations of the complexes prepared from the PEO 600 maleate gel (prepared as described in Experimental) support this view. The uncomplexed gel was a perfectly clear, translucent material shown by wide-angle X-ray analysis and d.t.a. to be completely amorphous. The complexed gel, however, showed a pronounced d.t.a. exotherm at 340K (6K min^{-1} heating rate) superimposed on a broad 'hump' (also observed in saturated linear complexes) as shown in *Figure 1E*. Henceforth, we identify the phase which disorders in the gel at ~340K as phase II and the principal crystalline phase in the linear PEO complexes melting at ~463K as phase I.

Thus the 325–340K endotherm in d.t.a. traces of linear sodium ion complexes is by implication, the disordering of phase II structures which form following the formation of phase I within the network of chains between the lamellae. Although phase II X-ray patterns have not been discerned in complexed gels, the absence of patterns characteristic of pure PEO in alt-containing or salt-free gels suggests that the 325–340K endotherm does not arise from melting of pure PEO in salt-containing or salt-free gels suggests that temperature of these endotherms. PEO crystals melting close to 340K would, of necessity, be large, discrete crystallites. Once-folded PEO 10000 melts at 337K, whereas the gel network is constructed from PEO 600 segments. The presence of phase II in excess salt samples suggests that phase II is a complexed phase differing in structure from phase I crystals and possibly requiring less conformational freedom of PEO chains for its formation than that required by phase I. The PEO–$LiCF_3SO_3$ complex discussed in our next paper also apparently forms well-defined phases I and II but with rather more (approximately 30%) of phase II than is formed by the sodium ion complexes. In this case, also, pure PEO lattice reflections are absent from the wide-angle X-ray diffractometer tracing. Further discussion of the structure of phase II is reserved for a following paper.

(ii) As reported previously, well-defined 'λ' transformations have been observed on the first d.t.a. heating cycle of a number of samples of PEO–NaI complexes (see *Figure 1F*). They are not so readily reproduced as the 325–340K endotherms, suggesting that a particular degree of structural order or morphological arrangement may be necessary for their observation. They have not been observed with PEO–NaSCN samples but have been observed with PEO–NH_4SCN with critical temperatures both below (334K) and above (375K) the

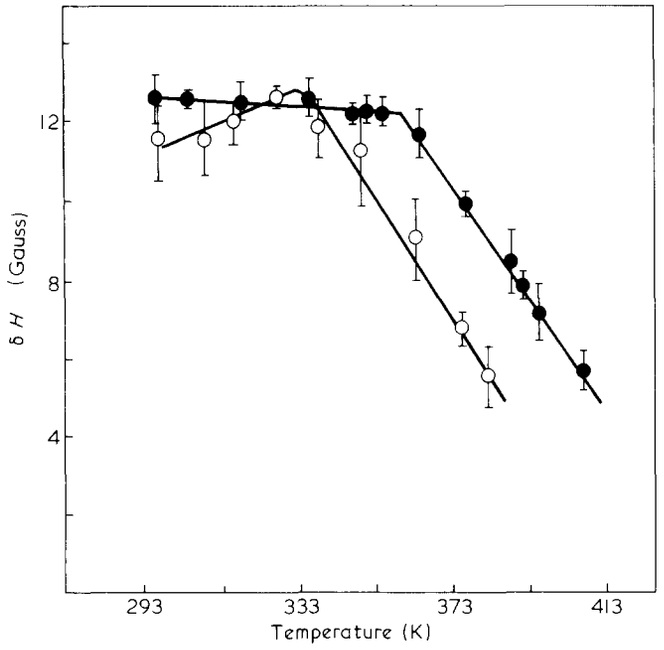

Figure 4 Temperature dependence of n.m.r. broadline width: ●, PEO 6 x 10^5—NaI; ○, PEO 6 x 10^5—NaSCN

normally-observed melting temperature (352K). In PEO–NaI complexes, observed critical temperatures range between 343 and 373K and they have not been observed at heating rates below 3K min^{-1}. Furthermore, they are not accompanied by 325–340K endotherms. However, the greater peak area of the λ transformation suggests that a disordering process within phase I may be involved. The largest λ-type endotherm observed amounted to ~14.7 kJ per mole EO corresponding to an entropy change of ~42 J mol^{-1} K^{-1} resulting in a larger overall entropy change than for melting alone, as anticipated in the discussion above.

The information given by broadline n.m.r. spectra of the complexes may be relevant to an understanding of the nature of the disordering process involved in the λ transformation. *Figure 4* (●) and (○) show the temperature dependence of the broadline component of the proton resonance spectrum for NaI and NaSCN complexes. At ambient temperatures the trace resembles that of a typical semicrystalline polymer with a broad component linewidth of ~12 gauss. A pronounced increase in intensity of the narrow component between 273K and ambient temperatures tends to support the conclusion drawn from d.t.a. that this represents the glass transformation range.

The width of the broadline component begins to decrease at ~330K for PEO–NaSCN and ~360K for PEO–NaI, equalling the narrow linewidth at ~423K for PEO–NaSCN and ~453K for PEO–NaI (extrapolated result). The latter temperatures approximate to those observed for the onset of lamellar thickening in the respective complexes.

The temperature of the onset of the line narrowing motion in NaI complexes occurs within the temperature range over which the λ transformations have been observed. (D.t.a. traces of samples not showing λ transformations often show ill-defined 'humps' over the temperature range of the line narrowing process.) While the morphological studies indicate that no large scale molecular translations occur over this temperature range, the n.m.r. results show that local rotational or translational displacements of PEO chain segments within phase I become possible.

Similar premelting disordering processes giving rise to d.t.a. endotherms and followed by narrowing of the n.m.r. broadline are known in other polymer systems such as PTFE[10] and the polyphosphazenes[11]. Poly[bis-(trifluorethoxy)phosphazene] shows a pronounced endotherm at ~363K and a small final melting endotherm at 513K; X-ray and n.m.r. analyses show that the endotherm at 363K represents a transformation to mesomorphic behaviour with enhanced side group and backbone mobility in crystalline regions. Both polymers apparently have rather stiff backbones.

The behaviour of PEO–NaI complexes exhibiting λ transformations is analogous to that of the polyphosphazenes. However, the absence of the 325–340K endotherm suggests that in these cases the disordering of phase II may be taking place with the cooperation of the disordering process in phase I. In any event, a single process of cooperative disordering throughout the system as a whole rather than an accumulation of local, independent transformations would seem to be required to account for the observations.

Conductivity measurements

The temperature dependence of alternating field conductivities of PEO–NaI and PEO–NaSCN complexes at frequencies of 10^2–10^5 Hz are plotted as log σ vs. $1/T$ in *Figures 5* and *6*. The plots in *Figures 5*(○, ●) and *6* are for crystalline, linear PEO complexes prepared with a nominally 1:4 stoichiometry; the sample giving the plot shown in *Figure 5* (△, ▲) contained excess NaI (1:3.2) in order to saturate the sample. Excess salt of 1:4 stoichiometry separates from the complexed material as crystals and may be observed by wide-angle X-ray diffraction and optical microscopy. As discussed above, lamellar thickening is suppressed in excess NaI samples. The plots in *Figures 5* (○, ●) and *6* for stoichiometric

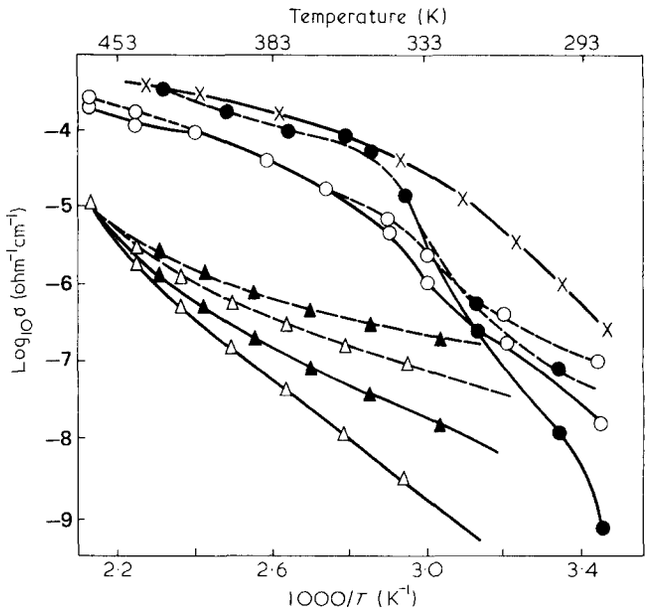

Figure 5 A.c. conductivities of PEO–NaI complexes: solid lines 10^2 Hz; dotted lines 10^5 Hz; open symbols solution deposited; filled symbols melt recrystallized. X, PEO 600—maleate gel—NaI (~1 : 6); ○, ●, PEO 10 000—stoichiometric complex (1 : 4); △, ▲, PEO 600 000—excess NaI (1 : 3.2)

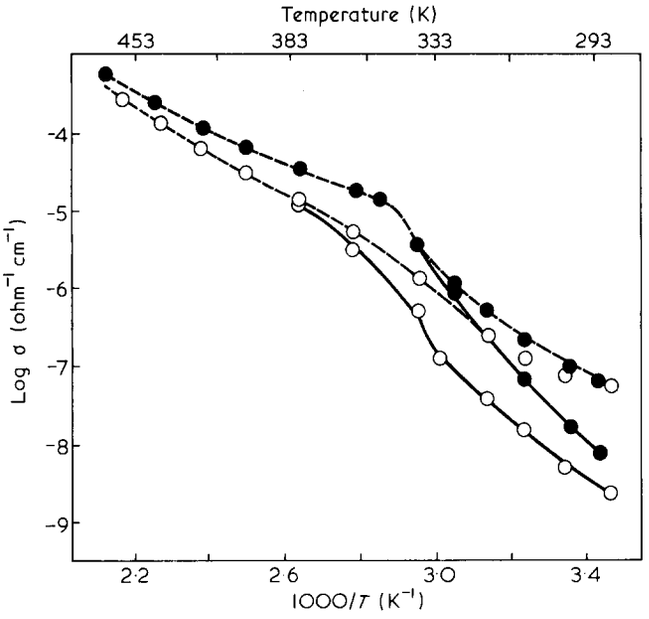

Figure 6 A.c. conductivities of PEO 10 000–NaSCN complexes: solid lines 10^2 Hz; dotted lines 10^5 Hz; open symbols solution deposited; filled symbols melt recrystallized

PEO 10 000 complexes are similar to those previously obtained[2] for 1:4 stoichiometric complexes with PEO 5×10^6 suggesting that the molecular weight of PEO is not a major influence on the form of the plots and the general level of conductivity.

Comparison between *Figures 5*(×) and *5*(○,●) shows that the major influence on conductivity from ambient temperatures to the melting temperature at ~463K is the concentration of complexed ion-pair (Schottky) vacancies. The concentration of such vacancies should have some dependence on temperature and the local stoichiometry as some ions vacate complexed sites and occupy interstitial spaces according to the equilibrium

$$\underset{(\mathrm{NaX})}{\text{Free salt}} + \underset{(n\mathrm{EO})}{\text{Vacant site}} \rightleftarrows \underset{(\mathrm{NaX}.n\mathrm{EO})}{\text{Complexed site}}$$

For phase I lamellae (80–90% of linear PEO samples) $n=4$, but in interlamellar regions the stoichiometry of phase II and non-crystalline sites is unknown. The free salt presumably resides in interlamellar or intermolecular pathways at lower temperatures in 1:4 stoichiometric samples. The suppression of complexed ion-pair vacancies in the saturated sample gives rise to the plot with monotonically increasing slope with decrease in $1/T$ as shown in *Figure 5*( ). This behaviour presumably reflects the increase in interstitial or intermolecular free volume with increase in temperature.

In contrast, linear crystalline samples with complexed ion-pair vacancies display two distinct regions of behaviour in their low frequency plots with a less steep gradient at higher temperatures. (The forms of the low frequency plots in *Figures 5*(○, ●) and *6* are similar to those reported by Wright[2] and by Armand *et al.*[3]. The latter prepared NaSCN–PEO samples with deficiencies of salt (1:4.5) so allowing a slightly greater conductivity than indicated in *Figure 6*.) The steeper, low temperature gradients in *Figures 5*(○,●) and *6* reflect the greater activation energies for the escape of ions from sites and for chain displacement resulting from the more stable association of cations with ether oxygens in the various types of coordination.

The two gradients are separated by a transition region which coincides with phase II melting and the onset of n.m.r. broad line narrowing. As discussed previously[2] the high temperature gradients are similar to those for pure PEO melts, corresponding to activation energies of ~55 kJ mol^{-1}. This suggests that in this region diffusion may be controlled by displacement of 'free' PEO chain segments. However, there is a steady increase in slope with temperature for NaSCN complexes above ~383K. This may reflect the increase in intermolecular free volume which permits the formation of bands in high molecular weight, annealed, solution-deposited samples.

The frequency dependence of σ at frequencies in the range 10^2–10^5 is an indication of structural inhomogeneity in the samples; polarization at the interface of two phases (1 and 2) occurs when:

$$\varepsilon_1 \sigma_{s1} \neq \varepsilon_2 \sigma_{s2}$$

where ε and σ_s are the permittivities and steady field (d.c.) conductivities respectively.*

Thus the saturated sample, in which the conducting paths may be essentially confined to the free volume between the complexed molecular structures, becomes homogeneous only at the final melting point of phase I lamellae. However, in the crystalline samples with complexed ion-pair vacancies, the pathways of high conductivity are apparently homogeneous to diffusion of the ions, or one kind of ion, at temperatures above the transition region, despite the obvious morphological heterogeneity conferred by the lamellar arrangements of the PEO chains. Thus melting of phase I lamellae would appear to be of less consequence to ionic diffusion in these samples. A slight increase in interfacial polarization in solution-deposited PEO 10 000–NaI at temperatures above ~443K is perhaps an indication of reduced accessibility of the higher conductivity pathways to a fraction of the ions following lamellar thickening. This process, which occurs in solution-deposited 1:4 PEO–NaI close to the melting point (but not in melt deposited samples), may allow an increase in the proportion of well-ordered crystalline material more remote from the lamellar surfaces. However, the conductivity of PEO 10 000–NaSCN gives no indication of similar morphological changes in this sample although in the previous discussion it is concluded that such changes do occur within the time allowed for temperature equilibrium in conductivity experiments.

The melt-deposited linear crystalline samples give consistently higher conductivities than solution-deposited samples except for the low temperature region of 1:4 NaI–PEO 10 000. The latter observation suggests that in this case, at least, improved electrode contact or

* For an inhomogeneous conductor consisting of alternate laminae only differing in d.c. conductivities, with the applied fields perpendicular to the laminae, the dimensionless step height of the dielectric relaxation is given by[12]:

$$\frac{\varepsilon_s - \varepsilon_\infty}{\varepsilon_\infty} = (p-1)^2 r/(p+r)^2$$

where ε_s and ε_∞ are the asymptotic values of the permittivity at low and high frequencies respectively, $p = \sigma_{s1}/\sigma_{s2}$ and r is the corresponding ratio of phase thicknesses. Thus the step height vanishes as $p \to 1$ or $r \to 0$.

compaction of melt samples does not provide an entirely satisfactory explanation. Moreover, increased vacancy concentration should not occur in the 'excess salt' sample. A greater degree of lattice imperfection in melt-crystallized samples could account, at least in part, for the enhanced conductivity. Such imperfections in melt crystallized samples might be expected according to the model for phase I crystals presented in a following paper.

The 1:6 NaI–PEO 600 maleate polyester network has an ambient temperature conductivity which lies on a continuous curve over the temperature range studied (*Figure 5*(△, ▲)). As discussed in the previous section, phase I crystalline complex is absent from this material. Phase II complex crystallites are present but apparently not in sufficient proportion to cause significant interfacial polarization or reduction of the level of conductivity at ambient temperatures to that of the linear complexes at low frequency.

However, the level of conductivity in the melt recrystallized NaI–PEO (1:4) sample at temperatures above the transition region is similar to that of the network. Since no crystallinity may exist in the network at these temperatures, the more complex morphology of the linear sample is apparently no great impediment to ionic diffusion over the higher temperature region. However, the removal of phase I crystallinity at least is seen to be a requirement for enhanced ambient temperature conductivity.

CONCLUSIONS

PEO–NaI and PEO–NaSCN are deposited from solutions into at least two distinct complexed phases. The peak of the melting endotherm for the high melting crystalline phase (phase I) occurs over the range 456–467K for complexes with PEO 6000 or greater and is independent of the nature of the anion. Phase II disorders over the range 325–340K and apparently exists within the network of conformationally-constrained chains in a PEO 600 maleate gel or in the interlamellar regions in the crystalline complexes.

At temperatures close to phase II disordering, the migration of the ionic components throughout the system commences. This gives rise to enhanced molecular motion of the PEO chains in phase I with narrowing of the n.m.r. broadline commencing at ~330K for NaSCN–PEO and 360K for NaI–PEO. λ-type exotherms with critical temperatures between 343 and 373K have been observed for NaI–PEO but not NaSCN–PEO. This temperature region also marks the transition from a high to a low activation energy for low frequency ionic conduction in samples with ion-pair vacancies.

All samples investigated were deposited from solutions with crystalline lamellae 150–200 Å in thickness. Annealing at temperatures above ~430K for NaSCN–PEO and ~450K for NaI–PEO gives rise to lamellar thickening of solution-deposited samples. Complexes with PEO 10000 or below form extended-chain lamellae of thickness ~450 Å. This process occurs rapidly close to the melting temperature so that the initial folded morphology may only be observed by d.t.a. at high heating rates. High molecular weight PEO complexes also partly thicken in the course of d.t.a. measurements, but annealed samples have lamellar thicknesses of ~600 Å. Lamellar thickening in NaI–PEO is prevented in saturated samples having excess NaI. The reduced concentration of ion-pair vacancies in these samples is also reflected in reduced ionic conduction and a different form for the $\log\sigma$ vs. $1/T$ plot, showing increasing activation energy with increasing temperature. These saturated samples also show interfacial polarization in a.c. fields at temperatures up to the phase I melting point whereas samples with ion-pair vacancies are virtually homogeneous to ion diffusion in the high temperature–low activation energy region.

The band morphologies of annealed solution-deposited high molecular weight PEO–NaSCN and the shish-kebab-like structures in melt recrystallized NaSCN complexes suggest that PEO–NaSCN has the more stable and rigid molecular unit which suffers less thermal disruption in the melt than the corresponding PEO–NaI unit. This is supported by the d.t.a. recrystallization temperatures and second (and subsequent) cycle melting temperatures which show that PEO–NaSCN samples recrystallize from the melt in the same extended or thickened conformations of the annealed solution-deposited samples. However, PEO–NaI with PEO molecular weights of 4000 or greater refold on recrystallization from the melt despite first cycle thickening of stoichiometric or salt deficient samples.

The absence of phase I in the PEO–maleate gel–NaI gives rise to an enhanced ambient temperature conductivity which lies on a plot which is continuous with the higher temperature–low activation energy region in the crystalline samples.

REFERENCES

1 Fenton, D. E., Parker, J. M. and Wright, P. V. *Polymer* 1973, **14**, 589
2 Wright, P. V. *Br. Polym. J.* 1975, **7**, 319
3 Armand, M., Chabagno, J. M. and Duclot, M. Presented at 2nd Int. Conf. on Solid Electrolytes, St. Andrews University, UK, 1978
4 Parker, J. M., Wright, P. V. and Lee, C. C. *Polymer* 1981, **22**, 1307
5 Lynch, A. C. *Proc. Inst. Elect. Eng.* (*B*) 1957, **104**, 363
6 Weber, G., Saenger, W., Vogtle, F. and Sieger, H. *Angew. Chem.* 1979, **18**, 226
7 Beech, D. R., Booth, C., Dodgson, D. V., Sharpe, R. R. and Waring, J. R. S. *Polymer* 1972, **13**, 73
Beech, D. R., Booth, C., Pickles, C. J., Sharpe, R. R. and Waring, J. R. S. *Polymer* 1972, **13**, 246
8 Lee, C. C. *PhD Thesis*, University of Sheffield (1979)
9 Moacanin, J. and Cuddihy, E. F. *J. Polym. Sci.* (*C*) 1966, **14**, 313
10 Matsushige, K., Enoshita, R., Ide, T., Yamauchi, N., Jaki, S. and Jakemura, T. *Jpn. J. Appl. Phys.* 1977, **16**, 681
11 Schneider, N. S., Desper, C. R., Singler, R. E., Alexander, M. N. and Sagalyn, P. L. 'Organometallic Polymers', (Ed. C. E. Carraher, Jr), Academic Press, 1978, pp. 271
12 Isard, J. O. *Proc. Inst. Elect. Eng.* (*B*) 1962, **109**, 440